

Scaling description of generalization with number of parameters in deep learning

Mario Geiger ^{* 1}, Arthur Jacot ^{* 2}, Stefano Spigler ¹, Franck Gabriel ², Levent Sagun ¹, Stéphane d’Ascoli ³, Giulio Biroli ³, Clément Hongler ², and Matthieu Wyart ¹

¹Institute of Physics, École Polytechnique Fédérale de Lausanne,
1015 Lausanne, Switzerland

²Institute of Mathematics, École Polytechnique Fédérale de
Lausanne, 1015 Lausanne, Switzerland

³Laboratoire de Physique Statistique, École Normale Supérieure,
PSL Research University, 75005 Paris, France

Abstract

We provide a description for the evolution of the generalization performance of fixed-depth fully-connected deep neural networks, as a function of their number of parameters N . In the setup where the number of data points is larger than the input dimension, as N gets large, we observe that increasing N at fixed depth reduces the fluctuations of the output function f_N induced by initial conditions, with $\|f_N - \bar{f}_N\| \sim N^{-1/4}$ where \bar{f}_N denotes an average over initial conditions. We explain this asymptotic behavior in terms of the fluctuations of the so-called Neural Tangent Kernel that controls the dynamics of the output function. For the task of classification, we predict these fluctuations to increase the true test error ϵ as $\epsilon_N - \epsilon_\infty \sim N^{-1/2} + \mathcal{O}(N^{-3/4})$. This prediction is consistent with our empirical results on the MNIST dataset and it explains in a concrete case the puzzling observation that the predictive power of deep networks improves as the number of fitting parameters grows. This asymptotic description breaks down at a so-called jamming transition which takes place at a critical $N = N^*$, below which the training error is non-zero. In the absence of regularization, we observe an apparent divergence $\|f_N\| \sim (N - N^*)^{-\alpha}$ and provide a simple argument suggesting $\alpha = 1$, consistent with empirical observations. This result leads to a plausible explanation for the cusp in test error known to occur at N^* . Overall, our analysis suggests that once

* Equal contribution

Correspondence: mario.geiger@epfl.ch, arthur.jacot@epfl.ch,
stefano.spigler@epfl.ch, franck.gabriel@epfl.ch, levent.sagun@epfl.ch,
stephane.dascalio@ens.fr, giulio.biroli@ens.fr, clement.hongler@epfl.ch and
matthieu.wyart@epfl.ch

models are averaged, the optimal model complexity is reached just beyond the point where the data can be perfectly fitted, a result of practical importance that needs to be tested in a wide range of architectures and data set.

1 Introduction

Deep neural networks are very successful at various tasks including image classification [25, 27] and speech recognition [19]. Yet, understanding why they work remains a challenge, and central questions need to be clarified.

- First, learning amounts to a descent in a high-dimensional loss landscape, which is a priori non-convex. What guarantees then that the dynamics does not get stuck in a poor minimum of the loss, leading to bad generalization?
- Second, deep networks tend to work in the over-parametrized regime where the number of parameters N can be (much) larger than the number of data points P which are used to optimize them. Thus, they are used in a regime where their capacity is very large (in the sense that they can still classify data even if the labels are randomized [42]), yet they generalize very well, at odds with the traditional VC-dimension learning theory.

Recent works suggest that these two questions are closely connected. Numerical and theoretical studies [17, 41, 20, 39, 9, 36, 37, 3, 30, 2, 18, 40] support that in the over-parametrized regime the loss landscape is not rough with isolated minima as initially thought [10, 8], but instead has connected level sets and presents many flat directions, even near its bottom. When optimizing neural networks using the hinge loss, there is a sharp phase transition (similar to the jamming transition that occurs in granular materials [21]) at some $N^*(P)$ such that for $N \geq N^*$ the dynamic process reaches global minima of the loss [18, 40]. In short, cranking up N guarantees low *training error*. A counter-intuitive aspect of deep learning is that increasing N above N^* does not destroy the predictive power by over-fitting the data, but instead appears to improve the *generalization performance* [34, 33, 4, 1]. Indeed the test error is observed to decrease in a slow power-law fashion [40] toward a limit as $N \rightarrow \infty$. Such a monotonic improvement is observed everywhere except near N^* , where the test error displays a cusp [1, 29, 40].

Explaining this observed dependence of the generalization on N in deep networks remains a challenge. In the perceptron, the simplest network without hidden layers, the cusp in the test error at the jamming point is also observed and predicted analytically [35, 12, 5, 26, 14, 13]. For deep linear networks trained with the mean-square loss, this cusp corresponds to an explosion of the norm of the output function precisely at $N = P$ [1, 29]. Yet, what controls its presence in non-linear deep networks that are trained with a descent dynamics is unclear. Another open question regards the asymptotic improvement of generalization

with N — a phenomenon that does not happen for perceptrons. Very recently, in the context of least-squares regression, this behavior was linked to the observed diminishing fluctuations of the output function with N [31]. Yet, what controls these fluctuations in deep non-linear networks and how they affect the test error in a classification task is not clear yet.

In this work, we address these questions using the recent discovery that in the limit $N \rightarrow \infty$, some deep learning models (in particular, fully-connected networks with any depth and a large class of non-linear functions that include the most common ones used in practice) are equivalent to a kernel method, where the kernel (coined the Neural Tangent Kernel or NTK) becomes deterministic and fixed at any finite time during training [22]. This result explains why generalization performance converges to a finite value as $N \rightarrow \infty$. Here, we use this framework to study the variation of the output function f_N at the end of training. For a fixed algorithm such variations are induced by the initial conditions. These variations still exist asymptotically for f_∞ [22], yet for a large data set, this effect appears to be subdominant even for the largest N we can reach. Departing from the $N \rightarrow \infty$ limit has two consequences. First, at finite N , the NTK will display a nonzero evolution in time, leading to a systematic difference between f_N and f_∞ . This effect on the performance is perceptible but small. Secondly, the NTK at initialisation has fluctuations around its mean that are of order $N^{-1/4}$, leading to similar variations for f_N which turn out to be dominant.

Next, by looking at the decision boundary, we argue that a variation in f of order δf increases the true test error by $\delta\epsilon \sim (\delta f)^2$. We use this asymptotic result to predict (i) the increase in generalization performance (decreased error $\epsilon_N - \epsilon_\infty$) obtained by ensemble averaging on n samples of the function f_N as n becomes large and (ii) the increase in generalization performance with N at fixed network depth. This description breaks down at the transition point N^* , where variations in f_N appear to diverge as a powerlaw, justifying the non-analyticity in the training error. We rationalize this divergence with a simple argument on a non-linear network trained with the hinge loss, that leads to $\|f_N\| \sim (N - N^*)^{-1}$. Overall, our work introduces a conceptual framework to describe how generalization error in deep learning evolves with the number of parameters. As an application, we demonstrate how ensemble averaging removes variations in the predictor and enhance generalization. Our result suggests that near-optimal generalization can be obtained by ensemble averaging networks that are slightly larger than N^* .

2 Improving generalization by averaging in MNIST

In this section we show how ensemble averaging improves generalization in networks that are slightly larger than the jamming transition N^* . We adopt the experimental setup of [40]. The task is to classify MNIST digits depending on their parity, where the standardized MNIST inputs are reduced to 10 dimensions using their first 10 PCA components. The architecture is a fully-connected

network with L layers, where each of the layers has h nodes. The non-linearity at each hidden layer is the standard rectified linear unit (ReLU). Weights of the network are initialized according to the random orthogonal scheme [38] and all biases are initialized to zero. The network is optimized using ADAM [24] with full batch and the learning rate is set to $\lambda = \min(10^{-1}h^{-1.5}, 10^{-4})$ ¹.

The network parametrizes an output function $f(x; \theta)$ with some parameters θ — the network’s weights and biases. The binary classification task consists in searching the parameters such that $\text{sign}f(x_\mu; \theta) = y_\mu$ for all MNIST images x_μ , where $y_\mu = \pm 1$ according to the parity of the digit depicted in the picture. To do so, we minimize the square-hinge cost function

$$C = \frac{1}{P} \sum_{\mu=1}^P \frac{1}{2} \max(0, \Delta_\mu)^2, \quad (1)$$

where $\Delta_\mu \equiv \epsilon_m - y_\mu f(x_\mu; \theta)$. In all of our simulations we fixed the margin ϵ_m to 1. The training process runs for a maximum of $2 \cdot 10^6$ steps². Typically, above jamming the training halts earlier as soon as the training reaches zero loss, while below jamming, training stalls at points with non-zero loss.

Our results, shown in Fig.1, demonstrate that after learning the test error has a peak near the transition at N^* , and then it slowly decreases as N becomes larger. We denote by \bar{f}_N^n the average of the function f_N over n different initial conditions. Remarkably, in our experiments ensemble-averaging over $n = 20$ independent runs led to a nearly flat test error for $N > N^*$; this supports that the improvement of generalization performance with N in this classification task originates from reduced variance of f_N when N gets large, as recently observed for mean-square regression [31]. An observation of potential practical interest is that near-optimal generalization is obtained by ensemble averaging slightly above N^* . *Thus the intuition that the most predictive and parsimonious models have just enough parameters to fit the data may indeed be correct, once one averages over differently initialized networks.*

3 Relationship between variance and generalization in classification tasks³

We consider an ensemble of functions f that approach pointwise a limiting function \bar{f} , so that $\delta f = f - \bar{f}$ satisfies $\|\delta f\|_\mu \ll \|f\|_\mu$ and $\langle \delta f \rangle = 0$, where the average is made on the ensemble considered. In what follows we define $\|f\|_\mu^2 = \int d\mu(x) f(x)^2$, where μ is some measure (empirically we shall use the

¹The exponent -1.5 has been empirically chosen so that the number of steps to converge is independent of h [22].

²Note that the number of steps and the number of epochs are the same in this setup.

³In spirit, this section shares some similarity with the bias variance decomposition developed in [11], except that we consider averaging on initial conditions instead of training set, and that we use the average output function as predictor, rather than apply the majority rule on a set of predictions.

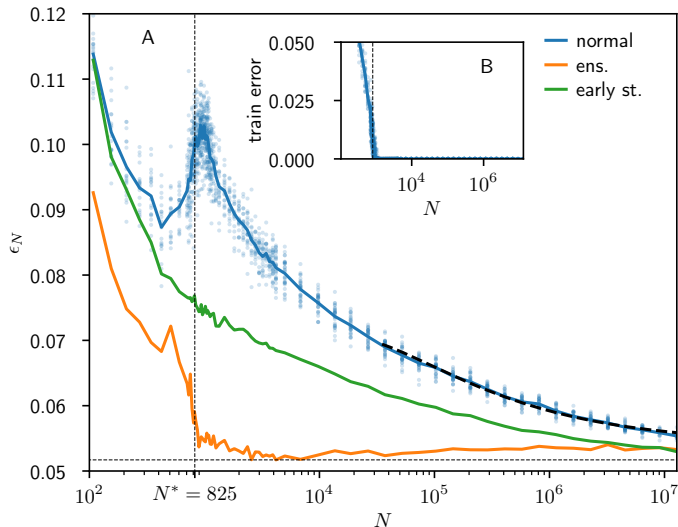


Figure 1: (A) Empirical test error *v.s.* number of parameters: average curve (blue, averaged over 20 runs); early stopping (green); ensemble average \bar{f}_N^n (orange) over $n = 20$ independent runs. In all the simulations we used fully-connected networks with depth $L = 5$ and input dimension $d = 10$, trained for $t = 2 \cdot 10^6$ epochs to classify $P = 10k$ MNIST images depending on their parity, using their first 10 PCA components, and the test set includes 50K images. The vertical dashed line corresponds to the jamming transition: at that point the test error peaks. Ensemble averaging leads to an essentially constant behavior when N becomes larger than N^* . The location of the jamming transition, N^* shown here, is measured in section 6 for extrapolated $t = \infty$. Black dashed line: asymptotic prediction of the form $\epsilon_N - \epsilon_\infty = B_0 N^{-1/2} + B_1 N^{-3/4}$, with $\epsilon_\infty = 0.054$, $B_0 = 6.4$ and $B_1 = -49$. (B) Training error *v.s.* number of parameters in MNIST data set.

uniform distribution on the training or test set or a Gaussian distribution on all x , all leading to similar results). For example, one may consider the ensemble of functions $\bar{f}_N^n = \frac{1}{n} \sum_{i=1}^n f_N^i$ obtained by varying initial conditions and averaging, or $\bar{f}_N = \lim_{n \rightarrow \infty} \bar{f}_N^n$. In this setup, the test errors of f and \bar{f}_N will be denoted respectively by ϵ and $\bar{\epsilon}_N$.

Consider a specific function f , and the two decision boundaries of f and \bar{f} defined as the set of inputs for which $f(x) = 0$ or $\bar{f}(x) = 0$. Consider a data point x_0 classified differently by these two functions — i.e. $f(x_0)\bar{f}(x_0) < 0$ — as illustrated in Fig.2. When the two boundaries are close enough, if the functions f and \bar{f} are smooth, the signed distance $\delta(x_0)$ between the two curves near x_0 must follow $\delta(x_0) = \delta f(x_0) / \|\nabla f(x_0)\| + \mathcal{O}(\delta f(x_0)^2)$, where $\delta f(x_0) = f(x_0) - \bar{f}(x_0)$. If the non-linearity in the network is itself smooth, smoothness of the output

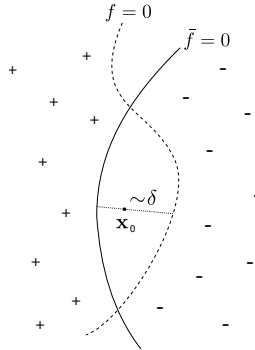


Figure 2: $f(x)$ and the limiting function $\bar{f}(x)$ (see Section 3) classify points according to their sign. They agree on the classification everywhere (\pm 's in the figure, where the functions are respectively both positive or both negative) except for the points that lie in between the two boundaries $f = 0$ and $\bar{f} = 0$. In the figure, let x be one such point, and δ is the typical distance from the boundary $f = 0$. In the limit where f and \bar{f} are close to each other, δ is of the same order of the distance between the two boundaries.

function is guaranteed both for N finite or not [22]. In the case of the Relu non-linear function, we show direct measurements of $\delta(x)$ in Appendix A supporting that this estimate still holds and become more and more accurate as $N \rightarrow \infty$.

Next we introduce the typical distance δ along the boundary:

$$\delta \equiv \langle |\delta f(x_0)| / \|\nabla f(x_0)\| \rangle_{x_0 \sim \text{test} \cap \text{interface}} \quad (2)$$

where the average is made over all the test data classified differently by f and \bar{f} . Such conditioning, however, does not affect the average. Indeed we have checked, as shown in Appendix A, that δ is very well estimated by $\|\delta f\|_\mu / \|\nabla f\|_\mu$ where μ indicates the uniform measure on all the test set. Next, we denote by $\Delta\epsilon$ the difference between the true test error of f and that of \bar{f} . It can be expanded by considering a small motion of the decision boundary B (that can consist of unconnected parts):

$$\Delta\epsilon = \int_B dx^{d-1} \left[\frac{\partial\epsilon}{\partial\delta(x)} \delta(x) + \frac{1}{2} \frac{\partial^2\epsilon}{\partial^2\delta(x)} \delta^2(x) + \mathcal{O}(\delta^3(x)) \right]. \quad (3)$$

Using that $\langle \delta(x) \rangle = \mathcal{O}(\delta f(x)^2)$ since $\langle \delta f(x) \rangle = 0$, we get that in average the true test error must increase quadratically with the norm of fluctuations δf :

$$\langle \Delta\epsilon \rangle \sim \delta^2 \sim \frac{\|\delta f\|_\mu^2}{\|\nabla f\|_\mu^2}. \quad (4)$$

Note that if the model \bar{f} displays a minimal true test error, the decision boundary is optimal: $\partial\epsilon/\partial\delta(x) = 0$ and $\partial^2\epsilon/\partial^2\delta(x) \geq 0$ for all $x \in B$, implying that the prefactor in Eq.4 must be positive⁴. If the true test error is small, the decision boundary will tend to be close to the ideal one, so that the prefactor in Eq.4 will still be positive. We expect it to be the case for the MNIST model we consider for which the test error is a few percents.

Eq.4 is a result on the ensemble average of the true test error. Yet, our data in Fig.1 supports that the test error is a self-averaging quantity: the test error of a given output function (blue points) lies close to its ensemble average (blue line). Such a self-averaging behavior is expected if there are many distinct regions where δ changes sign along the decision boundary. In what follows we will always consider averaged quantities, and drop the notation $\langle \rangle$.

⁴The pre-factor could be zero if the optimal boundary is degenerate, a situation that will not occur generically if the data have e.g. Gaussian noise.

4 Asymptotic generalization as $n \rightarrow \infty$

It is now straightforward to predict how an ensemble average of n networks behaves in the limit $n \rightarrow \infty$. The central limit theorem implies $\delta f \sim 1/\sqrt{n}$ while $\|\nabla f\|$ converges to some constant value. Thus $\delta \sim 1/\sqrt{n}$ and $\bar{\epsilon}_N^n - \bar{\epsilon}_N \sim 1/n$. These predictions are confirmed in Fig.3.

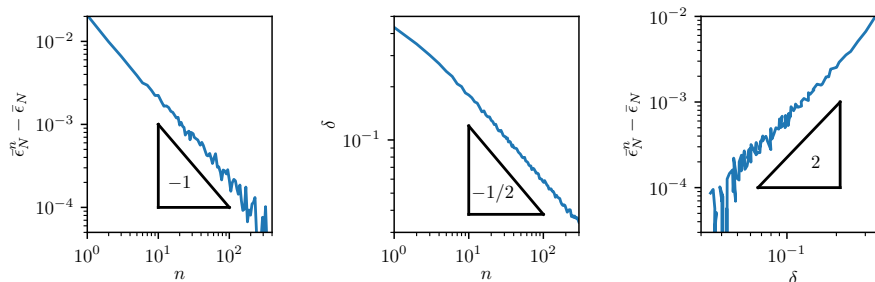


Figure 3: Left: increment of test error $\bar{\epsilon}_N^n - \bar{\epsilon}_N$ *v.s.* n , supporting $\bar{\epsilon}_N^n - \bar{\epsilon}_N \sim 1/n$. Center: δ as defined in Eq.2 *v.s.* number of average n , supporting $\delta \sim 1/\sqrt{n}$. Right: increase of test error $\bar{\epsilon}_N^n - \bar{\epsilon}_N$ as a function of the variation of the boundary decision δ , supporting the prediction $\bar{\epsilon}_N^n - \bar{\epsilon}_N \sim \delta^2$. Here $d = 30$, $h = 60$, $L = 5$, $N = 16k$ and $P = 10k$. The value $\bar{\epsilon}_N = 2.148\%$ is extracted from the fit.

5 Asymptotic generalization as $N \rightarrow \infty$

We now study the fluctuations of f_N^t throughout training for large networks using the Neural Tangent Kernel [22] or NTK. At initialization $t = 0$, $f_N^{t=0}$ is a random function whose limiting distribution as $N \rightarrow \infty$ is known to be Gaussian [32, 7, 28]. These types of fluctuations do not vanish as $N \rightarrow \infty$: the variance of $f_N^{t=0}$ at initialization is essentially constant in N .

However, as the network is trained, the learned part of the function dominates the randomness at initialization⁵. To understand why the fluctuations of the function at convergence $t \rightarrow \infty$ decrease with N , we must thus study the training process. The gradient descent dynamics of f_N^t is described by a kernel, the Neural Tangent Kernel Θ_N^t :

$$\Theta_N^t(x, x') = \sum_{k=1}^N \frac{d}{d\theta_k} f_N^t(x) \frac{d}{d\theta_k} f_N^t(x') \quad (5)$$

where $\frac{d}{d\theta_k} f_N^t$ is the derivative of the output of the network with respect to one parameter θ_k and the sum is over all the network's parameters. For a general

⁵In our setup, the output variance at initialization is smaller than one. Also, $P = 10k$ is large compared to $d = 10$. One could also suppress the randomness at initialization by training $f^{t=0} = f^t - f^{t=0}$.

cost $C(f) = \frac{1}{P} \sum_i c_i(f(x_i))$, the function follows the kernel gradient $\nabla_{\Theta_N^t} C|_{f_N^t}$ of the cost during training

$$\partial_t f_N^t(x) = -\nabla_{\Theta_N^t} C|_{f_N^t}(x) = -\frac{1}{P} \sum_i \Theta_N^t(x, x_i) c'_i(f_N^t(x_i)). \quad (6)$$

The NTK is random at initialization and varies during training. However as the number h of neurons in each hidden layer goes to infinity, the NTK converges to a deterministic limit $\Theta_N^t \rightarrow \Theta_\infty$ which stays constant throughout training [22]. In this limit, deep learning simply corresponds to a kernel method, and the only randomness of f_N^t at convergence $t \rightarrow \infty$ is due to the randomness at initialization. We shall see below that this effect is subdominant in the range of parameters we probe.

Other sources of variation of f come from the variation of the kernel itself, which occurs at finite N . It varies for two reasons. First, the kernel now evolves in time, in a trajectory that depends on initial conditions. It turns out however that this effect leads to small variations asymptotically. For any finite time T one finds [23]:

$$\|\Theta_N^{t=0} - \Theta_N^{t=T}\| = \mathcal{O}\left(\frac{1}{h}\right) = \mathcal{O}\left(N^{-1/2}\right). \quad (7)$$

Secondly, at finite N the kernel varies already at initialization:

$$\|\Theta_N^{t=0} - \Theta_\infty\| = \mathcal{O}\left(\frac{1}{\sqrt{h}}\right) = \mathcal{O}\left(N^{-1/4}\right). \quad (8)$$

The variation in Eq.8 decays much more slowly with N than that in Eq.7, and is thus expected to be the dominant source of the NTK fluctuations around Θ_∞ , as supported empirically below. Eq.8 can be readily obtained by re-writing Eq.5 as a sum on neurons and using the central limit theorem, as sketched in Appendix B and derived rigorously in [23].

Because the NTK describes the behaviour of the function f_N^t during training, and because the time to converge to a minimum of the loss converges to a constant as $N \rightarrow \infty$, from Eq.6 we expect the variance of the NTK to induce some variance of the same order to the function at the end of training. We confirm it is the case for the mean square loss in Appendix C. In conclusion for large enough width, the fluctuations of the kernel leads to fluctuations of $f_N^{t=\infty}$ of order $\mathcal{O}(N^{-1/4})$. This prediction is checked in Fig.4, supporting that $\|f_N - \bar{f}_N\| \sim N^{-1/4}$ in the range of N we can explore (eventually this curve must converge to a small constant $\|f_\infty - \bar{f}_\infty\|$, due to the finite fluctuations at initialization and the fact that we consider a large yet finite dataset [22]). In our setting observing this effect would require unreachable values of N , and we neglect this small constant). We expect that the same fluctuations that characterize f_N to also characterize ∇f_N , implying that $\|\nabla f_N\| = C_0 + C_1 N^{-1/4} + o(N^{-1/4})$. This result is consistent with our observations, as shown in Fig.5.A, in which we find empirically that C_1 is much larger than C_0 . We know that $\epsilon_N - \bar{\epsilon}_N \sim \delta_N^2$

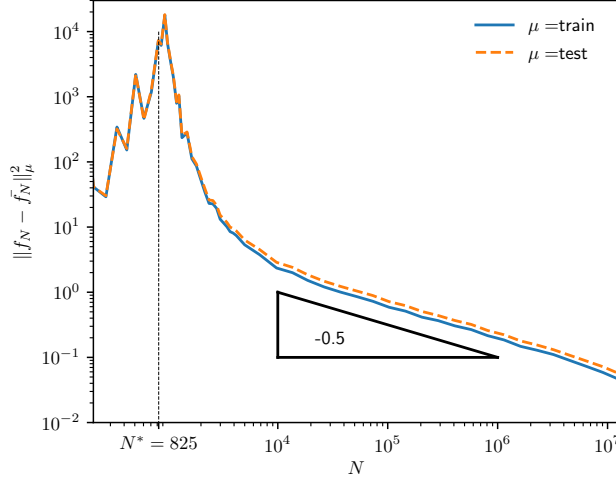


Figure 4: Variance of the output (averaged over $n = 20$ networks) *v.s.* number of parameters for different measures indicated in legend, showing a peak at jamming followed by a decay as N grows. Here $L = 5$, $d = 10$, $P = 10k$.

where δ_N indicates the typical distance between the decision boundaries $\bar{f}_N = 0$ and $f_N = 0$, as supported by Fig.5.B. The fluctuations of the decision boundary δ_N can be approximated as $\|f_N - \bar{f}_N\|/\|\nabla f_N\|$, as supported by Fig.5.C, leading to $\delta_N = A_0 N^{-1/4} + A_1 N^{-1/2} + o(N^{-1/2})$. We then obtain the key prediction $\epsilon_N - \bar{\epsilon}_N = B_0 N^{-1/2} + B_1 N^{-3/4}$. Since we measure both ϵ_N and $\bar{\epsilon}_N$ independently, we can test the prediction for the leading exponent without any fitting parameters, and indeed confirm that asymptotically $\epsilon_N - \bar{\epsilon}_N \sim N^{-1/2}$ as shown in Fig.5.D.

Finally we estimate the evolution of test error with N . We have:

$$\epsilon_N - \epsilon_\infty = (\epsilon_N - \bar{\epsilon}_N) + (\bar{\epsilon}_N - \bar{\epsilon}_\infty) + (\bar{\epsilon}_\infty - \epsilon_\infty) \quad (9)$$

The first term was estimated above, and turns out to be the dominant one for MNIST. The last term is independent of N , and should thus eventually dominate as $N \rightarrow \infty$. Yet as mentioned above, in the range of N we can explore the fluctuation of f_∞ around its mean are subdominant, implying that $(\bar{\epsilon}_\infty - \epsilon_\infty)$ is a small number. The middle term is very interesting, as it characterizes the possibility that deep nets do better than kernel methods at finite N . In that case features can be learned, in contrast with the situation at $N \rightarrow \infty$ for which the time evolution the activity of any hidden neuron becomes vanishingly small (yet important) [22]. In magnitude, this term corresponds to the distance between the yellow curve and its asymptote in Fig.1. For MNIST we observe that it is negative (learning features appears to improve generalization) for N larger than a few N^* , but the effect is small. We provide an argument why it may be so. For large N , we expect the difference between \bar{f}_N and \bar{f}_∞ to stem from (i) the

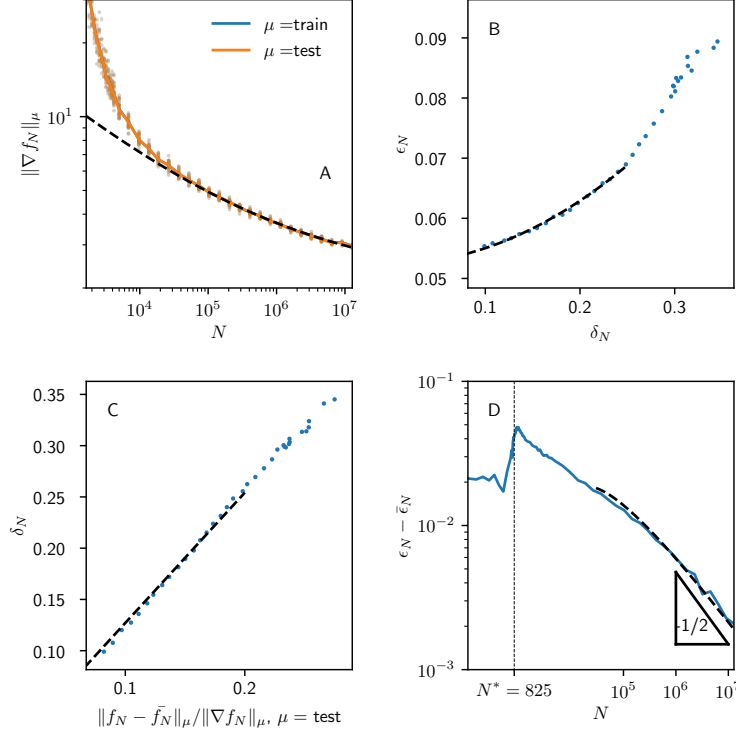


Figure 5: Here $L = 5$, $d = 10$, $P = 10k$. (A) The median of $\|\nabla f_N\|_\mu = \sqrt{\int d\mu(x) \|\nabla f_N(x)\|^2}$ over 20 runs (each appearing as a dot) is indicated as a full line. The dashed line correspond to our asymptotic prediction $\|\nabla f_N\| = C_0 + C_1 N^{-1/4}$ with $C_0 = 2.1$ and $C_1 = 51$. (B) Test error *v.s.* variation of the boundary, together with fit of the form $\epsilon_N = \epsilon_\infty + D_0 \delta_N^2$. (C) Variation of the boundary δ_N *v.s.* its estimate $\|f_N - \bar{f}_N\|_\mu / \|\nabla f_N\|_\mu$, well fitted by a linear relationship. (D) $\epsilon_N - \bar{\epsilon}_N$ *v.s.* N , with a fit of the form $\epsilon_N - \bar{\epsilon}_N = E_0 N^{-1/2} + E_1 N^{-3/4}$ with $E_0 = 7.6$ and $E_1 = -59$. If exponents in the fits are not imposed, we find for reasonable fitting ranges -0.28 instead of $-1/4$ in (A), 2.5 instead of 2 in (B), 1.1 instead of 1 in (C) and -0.42 instead of $-1/2$ in (D). Extracting exponents while also fitting for the location of the singularity, as is the case here for (A) and (B), leads to rather sloppy fits.

evolution of the kernel with time, described in Eq.7 and (ii) the fact that the relationship between the kernel and the function at infinite time is not linear, as described for the mean square loss in Eq.12. Both effects are $\mathcal{O}(N^{-1/2})$, i.e. much smaller than the $\mathcal{O}(N^{-1/4})$ fluctuations of f_N around its mean. The typical distance $\delta_{N,\infty}$ between the interfaces $\bar{f}_N = 0$ and $\bar{f}_\infty = 0$ is thus small

and $\mathcal{O}(N^{-1/2})$. According to Eq.3 we get:

$$\bar{\epsilon}_N - \bar{\epsilon}_\infty = \int_B dx^{d-1} \left[\frac{\partial \epsilon}{\partial \delta(x)} \delta_{N,\infty}(x) + \mathcal{O}(\delta_{N,\infty}^2(x)) \right] \quad (10)$$

Thus $\bar{\epsilon}_N - \bar{\epsilon}_\infty = \mathcal{O}(N^{-1/2})$, and thus cannot be neglected a priori. The fact that this term is small in practice presumably reflects that $\frac{\partial \epsilon}{\partial \delta(x)} \delta_{N,\infty}(x)$ often changes sign along the boundary, leading to a small pre-factor. Understanding if the situation can be different for well-chosen architectures, for which learning features would enhance significantly generalization accuracy is an important question for the future ⁶.

Overall, we get $\epsilon_N - \epsilon_\infty = B_0 N^{-1/2} + B_1 N^{-3/4}$, a form indeed consistent with observation as shown in Fig.1. Note that a direct fit of the test error *vs* N gives an apparent exponent smaller than $1/2$ [40], reflecting that (i) power-law fits are less precise when the value for the asymptote (here the value of ϵ_∞) is a fitting parameter and (ii) that correction to scaling needs to be incorporated for a good comparison with the theory (a fact that ultimately stems from the large correction to scaling of $\|\nabla f_N\|$ shown in Fig.5.A).

6 Vicinity of the jamming transition

The asymptotic description for generalization in the large N limit is not qualitatively useful for $N \leq N^*$, where a cusp in test error is found. We now argue that this cusp is induced by a singularity of $\|f_N\|$ at N^* when no regularization is used, as apparent in Fig.6.A. Indeed following our argument of Section 3, this effect must lead to singular fluctuations of the decision boundary at N^* , suggesting a non-analytical behavior for the true test error. This phenomenon shares some similarity with the norm divergence that occurs in linear networks with mean square loss for which $\|f_N\| \sim |N - P|^{-2}$ [1, 29]. Yet for losses better suited for classification such as the hinge loss, we argue that this explosion occurs at a different location with a different exponent.

Consider the hinge loss in Eq. 1. For $N \geq N^*$ the system is able to reach the ground state at $C = 0$, therefore all Δ_μ must be negative, i.e. all patterns must satisfy $y_\mu f(x_\mu) > \epsilon_m$. The parameter ϵ_m plays the role of a margin above which we are confident about the network's prediction. Because we do not use regularization on the norm $\|f\|$, the precise choice of ϵ_m does not affect N^* . Indeed the weights can always increase during learning so as to multiply f by any scalar λ , effectively reducing the margin by a factor $1/\lambda$, making the data easier to fit. By contrast, if a regularization is imposed to fix $\|f\| = \lambda$ (which may be hard to implement in practice), then N^* must be an increasing function of $\tilde{\epsilon}_m \equiv \epsilon_m/\lambda$. We assume that this function is differentiable in its argument around zero, a fact know to be true for the perceptron [16, 15],

⁶Very recently empirical results suggest that the test error can even increase for increasing and large N [6]. Yet, this observation was made in the teacher-student framework, where it is intuitively clear that the student should be penalized when its number of parameters becomes larger than the teacher.

thus $N^*(\tilde{\epsilon}_m) = N^*(0) + B_0\tilde{\epsilon}_m + o(\tilde{\epsilon}_m)$. Now consider our learning scheme (no regularization) for a network with $0 < N/N^*(0) - 1 \ll 1$, with initial conditions such that before learning $\|f_N^{t=0}\| = 1$. Initially, the effective margin is large with $\tilde{\epsilon}_m = 1$. Yet, all data can be fitted and the loss brought to zero if the norm increases so that $\tilde{\epsilon}_m \approx (N - N^*(0))/B_0$, corresponding to $\|f_N^t\| \sim (N - N^*)^{-1}$ where $N^* = N^*(0)$. At later times, the loss is zero and the dynamics stops.

This predicted inverse relation is tested in Fig.6.B. It is important to note that, as it is the case for any critical points, working at finite times cuts off a true singularity: as illustrated in Fig.6.B $\|f_N^t\|$ becomes more and more singular at long times. This effect also causes a shift of the transition N^* where the loss vanishes, that converges asymptotically to a well-defined value in the limit $t \rightarrow \infty$ as documented in [18]. N^* is therefore defined when $\|f_N^t\|$ displays a power law as function of $N/N^* - 1$.

Note that for other losses like the cross-entropy, the dynamics never stops completely but becomes extremely slow [2]. In such cases, we expect that asymptotically $\|f_N^t\| = \infty$ as soon as $N > N^*$, although this singularity should build up logarithmically slowly in time. For finite learning times we expect that a singularity will occur near N^* , but will be blurred as for the hinge loss if $t < \infty$.

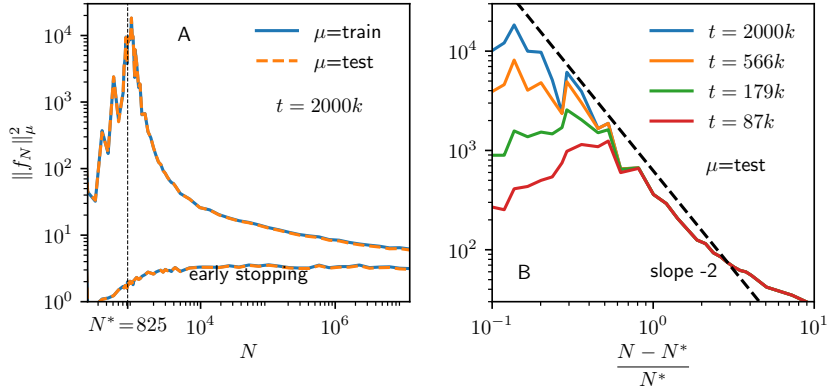


Figure 6: Here $L = 5$, $d = 10$, $P = 10k$. (A) $\|f\|^2 = \int d\mu(x)f(x)^2$ where for μ we took the uniform measure on the training and test set. We show the mean over the different realizations. Right after the jamming transition, the norm of the network diverges. (B) Same quantity computed after different learning times t as indicated in the legend, as a function of the distance from the transition. One observes that finite times cut off the divergence in the norm. The black line indicates a power-law with slope -2, that appears to fit the data satisfyingly. N^* has been fine tuned to obtain straight curves (power law behavior).

7 Conclusion

We have provided a description for the evolution of the generalization performance of by fixed-depth fully-connected deep neural networks, as a function of their number of parameters N . In the asymptotic regime of very large N , we find empirically that the network output displays reduced fluctuations with $\|f_N - \bar{f}_N\| \sim N^{-1/4}$. We have argued that this scaling behavior is expected from the finite N fluctuations of the Neural Tangent Kernel known to control the dynamics at $N = \infty$. Next we have provided a general argument relating fluctuations of the network output to decreasing generalization performance, from which we predicted for the test error $\epsilon_N - \epsilon_\infty = C_0 N^{-1/2} + C_1 N^{-3/4} + \mathcal{O}(N^{-1})$, consistent with our observation on MNIST. Overall this approach explains the surprising finding that generalization keeps improving with the number of parameters.

Secondly, we have argued that this description breaks down at $N = N^*$ below which the training set is not fitted. For the hinge loss where this jamming transition is akin to a critical point, and in the case where no regularization (such as early stopping) is used, we observe the apparent divergence $\|f_N\| \sim (N - N^*)^{-\alpha}$. We have argued, based on reasonable assumptions, that $\alpha = 1$, consistent with our observations. This predicted enhanced variance of f explains the spike in error observed at N^* .

On the practical side, our analysis suggests that optimal generalization does not require to take N much larger than N^* : since improvement of generalization with N stems from reduced variance in the output function, near-optimal generalization is readily obtained by performing an ensemble average of networks with N fixed, e.g. taken to be a few times N^* . Ensemble averaging is arguably more efficient than increasing N memory-wise. The usefulness of averaging breaks down near N^* where the variance of f is too large for efficient averaging. We thus recover the intuition that the optimal model complexity is reached just beyond the point where the data can be perfectly fitted, a result of practical importance that needs to be tested in a wide range of architectures and data set.

Acknowledgments

This work was partially supported by the grant from the Simons Foundation (#454935 Giulio Biroli, #454953 Matthieu Wyart). M.W. thanks the Swiss National Science Foundation for support under Grant No. 200021-165509. C.H. acknowledges support from the ERC SG Constamis, the NCCR SwissMAP, the Blavatnik Family Foundation and the Latsis Foundation.

References

- [1] Madhu S Advani and Andrew M Saxe. High-dimensional dynamics of generalization error in neural networks. *arXiv preprint arXiv:1710.03667*, 2017.
- [2] Marco Baity-Jesi, Levent Sagun, Mario Geiger, Stefano Spigler, Gerard Ben

- Arous, Chiara Cammarota, Yann LeCun, Matthieu Wyart, and Giulio Biroli. Comparing dynamics: Deep neural networks versus glassy systems. In Jennifer Dy and Andreas Krause, editors, *Proceedings of the 35th International Conference on Machine Learning*, volume 80 of *Proceedings of Machine Learning Research*, pages 314–323, Stockholmsmässan, Stockholm Sweden, 10–15 Jul 2018. PMLR.
- [3] Andrew J Ballard, Ritankar Das, Stefano Martiniani, Dhagash Mehta, Levent Sagun, Jacob D Stevenson, and David J Wales. Energy landscapes for machine learning. *Physical Chemistry Chemical Physics*, 2017.
- [4] Yamini Bansal, Madhu Advani, David D Cox, and Andrew M Saxe. Minnorm training: an algorithm for training over-parameterized deep neural networks. *CoRR*, 2018.
- [5] Siegfried Bös and Manfred Opper. Dynamics of training. In *Advances in Neural Information Processing Systems*, pages 141–147, 1997.
- [6] Lenaïc Chizat and Francis Bach. A note on lazy training in supervised differentiable programming. *arXiv preprint arXiv:1812.07956*, 2018.
- [7] Youngmin Cho and Lawrence K. Saul. Kernel methods for deep learning. In *Advances in Neural Information Processing Systems 22*, pages 342–350. Curran Associates, Inc., 2009.
- [8] Anna Choromanska, Mikael Henaff, Michael Mathieu, Gérard Ben Arous, and Yann LeCun. The loss surfaces of multilayer networks. In *Artificial Intelligence and Statistics*, pages 192–204, 2015.
- [9] Yaim Cooper. The loss landscape of overparameterized neural networks. *arXiv preprint arXiv:1804.10200*, 2018.
- [10] Yann N Dauphin, Razvan Pascanu, Caglar Gulcehre, Kyunghyun Cho, Surya Ganguli, and Yoshua Bengio. Identifying and attacking the saddle point problem in high-dimensional non-convex optimization. In *Advances in Neural Information Processing Systems*, pages 2933–2941, 2014.
- [11] Pedro Domingos. A unified bias-variance decomposition. In *Proceedings of 17th International Conference on Machine Learning*, pages 231–238, 2000.
- [12] Andreas Engel and Christian Van den Broeck. *Statistical mechanics of learning*. Cambridge University Press, 2001.
- [13] Silvio Franz, Sungmin Hwang, and Pierfrancesco Urbani. Jamming in multilayer supervised learning models. *arXiv preprint arXiv:1809.09945*, 2018.
- [14] Silvio Franz and Giorgio Parisi. The simplest model of jamming. *Journal of Physics A: Mathematical and Theoretical*, 49(14):145001, 2016.

- [15] Silvio Franz, Giorgio Parisi, Maxime Sevelev, Pierfrancesco Urbani, and Francesco Zamponi. Universality of the sat-unsat (jamming) threshold in non-convex continuous constraint satisfaction problems. *SciPost Physics*, 2(3):019, 2017.
- [16] Silvio Franz, Giorgio Parisi, Pierfrancesco Urbani, and Francesco Zamponi. Universal spectrum of normal modes in low-temperature glasses. *Proceedings of the National Academy of Sciences*, 112(47):14539–14544, 2015.
- [17] C Daniel Freeman and Joan Bruna. Topology and geometry of deep rectified network optimization landscapes. *International Conference on Learning Representations*, 2017.
- [18] Mario Geiger, Stefano Spigler, Stéphane d’Ascoli, Levent Sagun, Marco Baity-Jesi, Giulio Biroli, and Matthieu Wyart. The jamming transition as a paradigm to understand the loss landscape of deep neural networks. *arXiv preprint arXiv:1809.09349*, 2018.
- [19] Geoffrey Hinton, Li Deng, Dong Yu, George E Dahl, Abdel-rahman Mohamed, Navdeep Jaitly, Andrew Senior, Vincent Vanhoucke, Patrick Nguyen, Tara N Sainath, et al. Deep neural networks for acoustic modeling in speech recognition: The shared views of four research groups. *IEEE Signal processing magazine*, 29(6):82–97, 2012.
- [20] Elad Hoffer, Itay Hubara, and Daniel Soudry. Train longer, generalize better: closing the generalization gap in large batch training of neural networks. In *Advances in Neural Information Processing Systems*, pages 1729–1739, 2017.
- [21] Andrea J Liu, Sidney R Nagel, W Saarloos, and Matthieu Wyart. *The jamming scenario - an introduction and outlook*. OUP Oxford, 06 2010.
- [22] Arthur Jacot-Guillarmod, Franck Gabriel, and Clement Hongler. Neural tangent kernel: Convergence and generalization in neural networks. In *Advances in Neural Information Processing Systems 31*, pages 8580–8589. 2018.
- [23] Arthur Jacot-Guillarmod, Franck Gabriel, and Clement Hongler. The neural tangent kernel describes the hessian of overparametrized dnns. 2019.
- [24] Diederik P Kingma and Jimmy Ba. Adam: A method for stochastic optimization. *International Conference on Learning Representations*, 2015.
- [25] Alex Krizhevsky, Ilya Sutskever, and Geoffrey E Hinton. Imagenet classification with deep convolutional neural networks. In *Advances in neural information processing systems*, pages 1097–1105, 2012.
- [26] Yann Le Cun, Ido Kanter, and Sara A Solla. Eigenvalues of covariance matrices: Application to neural-network learning. *Physical Review Letters*, 66(18):2396, 1991.

- [27] Yann LeCun, Yoshua Bengio, and Geoffrey Hinton. Deep learning. *Nature*, 521(7553):436, 2015.
- [28] Jae Hoon Lee, Yasaman Bahri, Roman Novak, Samuel S. Schoenholz, Jeffrey Pennington, and Jascha Sohl-Dickstein. Deep neural networks as gaussian processes. *ICLR*, 2018.
- [29] Zhenyu Liao and Romain Couillet. The dynamics of learning: A random matrix approach. *arXiv preprint arXiv:1805.11917*, 2018.
- [30] Zachary C Lipton. Stuck in a what? adventures in weight space. *International Conference on Learning Representations*, 2016.
- [31] Brady Neal, Sarthak Mittal, Aristide Baratin, Vinayak Tantia, Matthew Scicluna, Simon Lacoste-Julien, and Ioannis Mitliagkas. A modern take on the bias-variance tradeoff in neural networks. *arXiv preprint arXiv:1810.08591*, 2018.
- [32] Radford M. Neal. *Bayesian Learning for Neural Networks*. Springer-Verlag New York, Inc., Secaucus, NJ, USA, 1996.
- [33] Behnam Neyshabur, Zhiyuan Li, Srinadh Bhojanapalli, Yann LeCun, and Nathan Srebro. Towards understanding the role of over-parametrization in generalization of neural networks. *arXiv preprint arXiv:1805.12076*, 2018.
- [34] Behnam Neyshabur, Ryota Tomioka, Ruslan Salakhutdinov, and Nathan Srebro. Geometry of optimization and implicit regularization in deep learning. *arXiv preprint arXiv:1705.03071*, 2017.
- [35] David Saad and Sara A Solla. On-line learning in soft committee machines. *Physical Review E*, 52(4):4225, 1995.
- [36] Levent Sagun, Léon Bottou, and Yann LeCun. Singularity of the hessian in deep learning. *International Conference on Learning Representations*, 2017.
- [37] Levent Sagun, Utku Evci, V. Uğur Güney, Yann Dauphin, and Léon Bottou. Empirical analysis of the hessian of over-parametrized neural networks. *ICLR 2018 Workshop Contribution*, *arXiv:1706.04454*, 2017.
- [38] Andrew M Saxe, James L McClelland, and Surya Ganguli. Exact solutions to the nonlinear dynamics of learning in deep linear neural networks. *International Conference on Learning Representations*, 2014.
- [39] Daniel Soudry and Yair Carmon. No bad local minima: Data independent training error guarantees for multilayer neural networks. *arXiv preprint arXiv:1605.08361*, 2016.
- [40] Stefano Spigler, Mario Geiger, Stéphane d’Ascoli, Levent Sagun, Giulio Biroli, and Matthieu Wyart. A jamming transition from under-to over-parametrization affects loss landscape and generalization. *arXiv preprint arXiv:1810.09665*, 2018.

- [41] Luca Venturi, Afonso Bandeira, and Joan Bruna. Neural networks with finite intrinsic dimension have no spurious valleys. *arXiv preprint arXiv:1802.06384*, 2018.
- [42] Chiyuan Zhang, Samy Bengio, Moritz Hardt, Benjamin Recht, and Oriol Vinyals. Understanding deep learning requires rethinking generalization. *International Conference on Learning Representations*, 2017.

A Robustness of the boundaries distance $\delta(x)$ estimate

Fig.7 shows that the linear estimate for the distance $\delta(x)$ between two decision boundaries, $\delta(x) = \delta f(x)/\|\nabla f(x)\|$, holds for Relu nonlinear function and improves as $N \rightarrow \infty$.

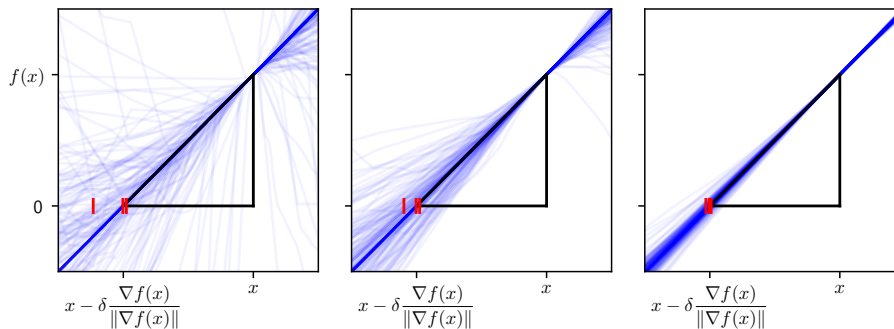


Figure 7: Value of the output function f , in the direction of its gradient starting from x . Here 200 curves are shown, corresponding to 200 data x in the test set within the decision boundaries $f_N = 0$ and $\bar{f}_N = 0$ — i.e. $f_N(x)\bar{f}_N(x) < 0$. If the linear prediction is exact, then we expect $f(x - \delta \frac{\nabla f(x)}{\|\nabla f(x)\|}) = 0$ where $\delta = \delta f(x)/\|\nabla f(x)\|$. This prediction becomes accurate for large N . To make this statement quantitative, The 25%, 50%, 75% percentile of the intersection with zero are indicated with red ticks. Even for small N the interval between the ticks is small, so that the prediction is typically accurate. From left to right $N = 938, 13623, 6414815$. Here $d = 10, L = 5$ and $P = 10k$.

Fig.8 demonstrates the validity of the estimate of the typical distance between two boundary decisions presented in the main text $\delta \sim \|\delta f\|_\mu / \|\nabla f\|_\mu$, where μ corresponds to the uniform measure on all the test points.

B Central limit theorem of the NTK

In this section, we present a heuristic for the finite-size effects that are displayed by the NTK at initialization: informally, this is the central limit theorem counterpart to the NTK asymptotic result, which can be viewed as a law of large numbers. A rigorous derivation, including the behavior during training, is beyond the scope of this paper and will be presented in[23].

The NTK (see Eq.5) can be re-written as:

$$\sum_{\alpha} \left[1 + \frac{1}{h} \sum_{\beta \in v^-(\alpha)} a_{\beta}(x) a_{\beta}(x') \right] \left[g'(b_{\alpha}(x)) g'(b_{\alpha}(x')) \frac{\partial f(x)}{\partial a_{\alpha}} \frac{\partial f(x')}{\partial a_{\alpha}} \right] \quad (11)$$

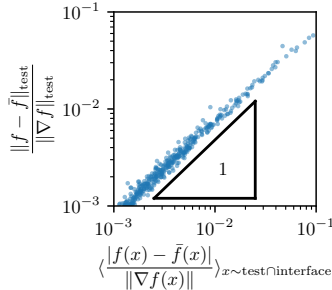


Figure 8: Test for the estimate of the distance δ between the boundary decision of f and \bar{f} . Each point is measured from a single ensemble average of various sizes. Here $d = 30$, $h = 60$, $L = 5$, $N = 16k$ and $P = 10k$.

where $a_\alpha(x) = g(b_\alpha(x))$ is the activity of neuron α when data x is shown, while $b_\alpha(x)$ is its pre-activity and $v^-(\alpha)$ is the set of h neurons in the layer preceding α . The first bracket converges to a well-defined limit described by a so-called activation kernel, see [32, 7, 22] which use a law of large numbers to prove this fact. The second bracket has fluctuations of order of its mean. The normalization is chosen such that each layer contributes a finite amount to the kernel, so that the mean is of order $1/h$. For a given hidden layer, the contributions of two neurons can be shown to have a covariance that is positive and decays as $1/h^3$, and thus does not affect the scaling expected from the central limit theorem for uncorrelated variables. For a rectangular network, this suggests that fluctuations associated with the contribution of one layer to the kernel is of order $1/\sqrt{h} \sim N^{-1/4}$.

C Fluctuations of output function for the mean square error loss

In this section, we discuss the fluctuations of the output function after training for the mean square error loss: $C(f) = \frac{1}{2P} \sum_i |y_i - f(x_i)|^2$. We first investigate the variance of f_N^t in the limit $N \rightarrow \infty$, then we explain the deviations due to finite size effects, at last we discuss the hing loss case.

C.1 Infinite width

Let us first study the variance of f_N^t in the limit $N \rightarrow \infty$. In this limit the function $f_\infty^{t=0}$ at initialization follows a centered Gaussian distribution described by a covariance kernel Σ . During training however, the dynamics of f_∞^t is

described by a deterministic kernel $\Theta_\infty^{(L)}$, the Neural Tangent Kernel (NTK):

$$\partial_t f_\infty^t(x) = \frac{1}{P} \sum_i \Theta_\infty(x, x_i) (y_i - f_\infty^t(x_i)).$$

If the NTK is positive definite (which is proven when the inputs all lie on the unit circle and the non-linearity is not a polynomial), the network reaches a global minimum at the end of training $t \rightarrow \infty$. In particular the values of the function on training set are deterministic: $f_\infty^{t=\infty}(x_i) = y_i$. The values of the function outside the training set can be studied using the vector of values of f_∞^t on the training set $\tilde{y}^t = (f_\infty^t(x_i))_{i=1, \dots, P}$. Denoting by $\tilde{\Theta}_\infty = (\Theta_\infty(x_i, x_j))_{ij}$ the empirical Gram matrix:

$$y = \tilde{y}^{t=\infty} = \tilde{y}^{t=0} + \frac{1}{P} \int_0^\infty \tilde{\Theta}_\infty (y - \tilde{y}^t) dt,$$

so that

$$\frac{1}{P} \int_0^\infty (y - \tilde{y}^t) dt = \tilde{\Theta}_\infty^{-1} (y - \tilde{y}^{t=0}) = \tilde{\Theta}_\infty^{-1} y - \tilde{\Theta}_\infty^{-1} \tilde{y}^{t=0}.$$

These two terms represent the fact that the network needs to learn the labels y and forget the random initialization. We can therefore give a formula for the values outside the training set, using the vector $\tilde{\Theta}_{\infty, x} = (\Theta_\infty(x, x_i))_{i=1, \dots, P}$:

$$\begin{aligned} f_\infty^t(x) &= f_\infty^{t=0}(x) + \tilde{\Theta}_{\infty, x} \frac{1}{P} \int_0^\infty (y - \tilde{y}^t) dt \\ &= f_\infty^{t=0}(x) - \tilde{\Theta}_{\infty, x} \tilde{\Theta}_\infty^{-1} \tilde{y}^{t=0} + \tilde{\Theta}_{\infty, x} \tilde{\Theta}_\infty^{-1} y. \end{aligned}$$

The first two terms are random, but they partly cancel each other, their sum is a centered Gaussian distribution with zero variance on the training set and a small variance for points close to the training set: the more training data points used, the lower the variance at initialization. The last term is equal to the kernel regression on y with respect to the NTK, it is not random.

This shows that even in the infinite-width limit, $f_\infty^{t=\infty}$ has some variance which is due to the variance of $f_\infty^{t=0}$ at initialization. Yet, in the setup where the number of data points is large enough, the variance due to initialization almost vanishes during training and the scaling of the variance due to finite-size effects in N will appear in the last term.

C.2 Finite width

For a finite width N , the training is also described by the NTK Θ_N^t which is random at initialization and varies during training because it depends on the parameters. The integral formula becomes

$$f_N^t(x) = f_N^{t=0}(x) + \int_0^\infty \tilde{\Theta}_{N, x}^t (y - \tilde{y}^t) dt$$

However the noise at initialization is $\Omega(N^{-1/4})$, whereas the rate of change is only $\Omega(N^{-1/2})$ [23], we can therefore make the approximation

$$f_N^t(x) = f_N^{t=0}(x) + \tilde{\Theta}_{N,x}^{t=0} \int_0^\infty (y - \tilde{y}^t) dt + \mathcal{O}(N^{-1/2}).$$

Assuming that there are enough parameters such that the Gram matrix $\tilde{\Theta}_N^{t=0}$ is invertible, we can again decompose the integral into two terms:

$$\int_0^\infty (y - \tilde{y}^t) dt = \tilde{\Theta}_N^{-1} y - \tilde{\Theta}_N^{-1} \tilde{y}^{t=0} + \mathcal{O}(N^{-1/2}),$$

such that

$$f_N^t(x) = f_N^{t=0}(x) - \tilde{\Theta}_{N,x}^{t=0} \tilde{\Theta}_N^{-1} \tilde{y}^{t=0} + \tilde{\Theta}_{N,x}^{t=0} \tilde{\Theta}_N^{-1} y + \mathcal{O}(N^{-1/2}). \quad (12)$$

Here again the first two terms almost cancel each other, but the third term is random due to the randomness of the NTK which is of order $\mathcal{O}(N^{-1/4})$, as needed.

C.3 Hinge Loss

For the hinge loss set-up, we do not have such a strong constraint on the value of the function $f_N^{t=\infty}$ on the training set $\tilde{y}^{t=\infty}$ as for regression, but we still know that they must satisfy the margin constraints

$$\tilde{y}_i^{t=\infty} y_i > 1.$$

The vector $\tilde{y}^{t=\infty}$ is therefore random for the hinge loss as a result of the random initialization of $f_N^{t=0}$ and the fluctuations of the NTK. Again it is natural to assume the first type of fluctuations to be subdominant and the second type to be of order $\mathcal{O}(N^{-1/4})$.